

1 **Weddell Sea anomalies: Excitation, propagation, and**
2 **possible consequences**

H. H. Hellmer, F. Kauker[‡], R. Timmermann

3 Department of Climate Science, Alfred Wegener Institute for Polar and
4 Marine Research, Bremerhaven, Germany

5 [‡] and O.A.Sys, Ocean Atmosphere Systems, Hamburg, Germany

H. H. Hellmer, Department of Climate Science, Alfred Wegener Institute for Polar and Marine Research, Bussestr. 24, D-27570 Bremerhaven, Germany. (Hartmut.Hellmer@awi.de)

F. Kauker, Department of Climate Science, Alfred Wegener Institute for Polar and Marine Research, Bussestr. 24, D-27570 Bremerhaven, (Frank.Kauker@awi.de), and O.A.Sys, Ocean Atmosphere Systems, Schanzenstr. 36, D-20357 Hamburg, Germany. (frank@oasys-research.de)

R. Timmermann, Department of Climate Science, Alfred Wegener Institute for Polar and Marine Research, Bussestr. 24, D-27570 Bremerhaven, Germany. (Ralph.Timmermann@awi.de)

6 Antarctic marginal seas are susceptible to significant decadal variability
7 as revealed by the analysis of a 200-year integration of a regional ice-ocean
8 model forced with the atmospheric output of the IPCC climate model ECHAM5-
9 MPIOM. The strongest signal occurs on the southern and western Weddell
10 Sea continental shelf where changes in bottom salinity are initiated by a vari-
11 able sea ice cover and modification of surface waters near the Greenwich merid-
12 ian. Related zonal shifts of the western rim current guide deep waters with
13 different temperature out of the Weddell Sea. With a deep boundary cur-
14 rent the temperature signal propagates westward through southern Drake
15 Passage and along the upper continental rise in the southeast Pacific thereby
16 influencing the hydrographic conditions on the continental shelf of Belling-
17 shausen, Amundsen, and Ross Seas.

1. Introduction

18 The Southern Ocean represents an essential component of the global climate system.
19 Inter alia, its interaction with the floating extensions of the Antarctic ice sheet creates
20 water masses fueling the lower branch of the global meridional overturning circulation.
21 A +40-year time series from the Ross Sea reveals long-term changes of shelf water char-
22 acteristics [*Jacobs et al.*, 2002]. The continuous salinity decrease since the early 1960s
23 might have changed the bottom water characteristics further to the west [*Rintoul*, 2007].
24 Reasons for the decrease are still debated: (1) an increased freshwater input due to ice
25 shelf basal melting in Amundsen and Bellingshausen Seas [*Rignot and Jacobs*, 2002] or (2)
26 a sampling-aliasing of a recurring salt anomaly initiated at the continental slope of the
27 Amundsen Sea [*Assmann and Timmermann*, 2005]. The Ross Sea freshening coincides
28 with a positive trend of the Southern Annular Mode (SAM) which can be linked to a
29 strengthening and poleward shift of the westerly winds [*Thompson and Solomon*, 2002],
30 enhanced upwelling of relatively warm Circumpolar Deep Water (CDW) onto the Antarc-
31 tic continental shelf [*Walker et al.*, 2007], and thus increased ice shelf basal melting in the
32 Pacific sector. Changes on shorter time scales were observed for the deep waters in the
33 Weddell Sea [*Gordon*, 1982; *Fahrbach et al.*, 2004]. The earlier cooling can be related to
34 the occurrence of the Weddell Polynya and might have spread to the north as far as the
35 Argentine Basin [*Coles et al.*, 1996]. A link between the Weddell Sea and the seas west of
36 the Antarctic Peninsula is still on dispute. A narrow boundary current in southern Drake
37 Passage [*Naveira Garabato*, 2003; *Tarakanov et al.*, 2008] which, according to geological
38 records [*Hillenbrand et al.*, 2008], sets southwest on the upper continental rise west of the

39 Antarctic Peninsula has been postulated only recently. Therefore, the southeast Pacific
40 Ocean is still considered solely as intensifier and radiator of ocean variability generated
41 in the southern hemisphere [e.g., *Beckmann and Timmermann, 2001*].

2. Method

42 We investigate the results of the coupled ice-ocean model BRIOS-2.2 [*Timmermann et*
43 *al., 2002*], which resolves the Southern Ocean on a grid of 1.5° zonally and $1.5^\circ \times \cos \phi$
44 meridionally (~ 80 km in southern Drake Passage). The model is forced for 200 years
45 (1900–2099) with the atmospheric output of the IPCC-20C3M scenario simulation of the
46 coupled atmosphere–sea ice–ocean ECHAM5-MPIOM [*Roeckner, 2004*]. The latter scored
47 best in an Antarctic assessment of IPCC AR4 coupled models [*Connolly and Bracegirdle,*
48 *2007*]. Because no spin-up was performed to reach a quasi-stationary state, the first 20
49 years (1900–1919) were discarded from the analysis. Seasonal and interannual variability
50 was eliminated by considering annual means and applying a 5-year running mean filter,
51 respectively. Trends were removed. The unfiltered time series contains one event, lasting
52 for about 40 years, around the turn of the century which cannot be associated with the
53 mechanisms proposed below. The analysis of the unfiltered data reveals essentially the
54 same results; for a better presentation, however, we removed the longest time-scales by
55 subtracting the 20-year running mean. In addition, in two sensitivity runs the atmospheric
56 forcing in the Weddell Sea sector ($60^\circ\text{W} - 60^\circ\text{E}$) was altered by monthly mean composites
57 of surface winds, 2 m-temperature, and dew point temperature from post-2000 years of
58 extreme high and low bottom salinities in the south/western Weddell Sea, preceding

59 the bottom salinity by 5 years (lower panel in Fig. 1; for more information see auxiliary
60 material).

3. Results

61 EOF-analyses of the model output for different variables and levels reveals a prominent
62 mode for bottom salinity (S_{bot}) in the southern and western Weddell Sea (Fig. 1). The
63 largest amplitude of this leading EOF-mode (48% described variance) amounts to about
64 0.03, corresponding to a peak-to-peak salinity range of 0.1. These changes in S_{bot} are
65 significantly correlated ($r = 0.56$) with the ECHAM5-MPIOM's SAM index for S_{bot} lagging
66 SAM by five years (Fig. 1). We defined the SAM index as the leading EOF of the annual
67 mean sea level pressure (SLP) south of 20°S. Its distribution agrees well with published
68 SAM patterns (e.g., Fig. 1 in *Lefebvre et al.* (2004)). The leading S_{bot} -EOF pattern
69 covers the western Weddell Sea continental shelf and upper slope up to the tip of the
70 Antarctic Peninsula (Fig. 1). A regression of the bottom velocities u and v on the leading
71 S_{bot} -EOF time series (pc_1) shows that the highest correlation ($r_{max} = 0.85$) extends from
72 the Weddell basin's western rim current into the southeast Pacific sector of the Southern
73 Ocean. This strong correlation is also evident for the barotropic transport streamfunction
74 (Ψ) regressed on pc_1 (Fig. 2), indicating the dominance of the bottom signal in the whole
75 water column. A lagged-regression of the same quantities shows a maximum regression
76 slope in the eastern Bellingshausen Sea for pc_1 leading the barotropic transport by four
77 years. Within eight years the area of strong correlation ($r > 0.5$) between pc_1 and Ψ
78 propagates westward along the continental slope until it fades approaching $\sim 75^\circ\text{E}$ (Fig.
79 2). The overlap of positive correlation with an 8-year lag and negative correlation ($r < -$

80 0.5) with a 0-year lag in Amundsen and Ross Seas indicates a 16-year periodicity for the
81 westward propagating anomaly generated in the Weddell Sea. The periodicity is triggered
82 by the approximately 16-year cycle of the ECHAM5-MPIOM's SAM forcing (Fig. 1).

83 The lag-correlation between circumpolar bottom temperature (T_{bot}) and the first EOF
84 of S_{bot} shows a very similar pattern in space and intensity as for the barotropic transport
85 streamfunction, although of opposite sign ($r_{max} = -0.85$ for lag 0 years). T_{bot} exhibits
86 maximum variability for lag +4 years at the southeast Pacific continental slope (Fig. 2)
87 corresponding to temperature changes of up to 0.32 °C. A meridional section at 81°W
88 (not shown) exhibits a vertical dipole at the continental slope with negative correlation
89 ($r = -0.7$) in the 1000–3000 m depth range and positive correlation ($r = 0.5$) above. The
90 dipole pattern suggests the deep signal being advected into the southeast Pacific Ocean
91 rather than formed locally by atmosphere–ice–ocean interaction and deep convection. The
92 deep temperature signal advances westward and onto the continental shelf without losing
93 much of its intensity as it approaches the fringes of the West Antarctic Ice Sheet. For
94 the 16-year period the squared coherency [*v.Storch and Zwiers, 2003*] between pc_1 and the
95 modeled meltwater fluxes from these ice shelves is 0.5 at a significance level close to 90%.
96 For lag +8 years (not shown) the anomaly enters the Ross Sea continental shelf at 180°
97 with a correlation of $r > 0.5$ but fades as it reaches the western edge of the Ross Ice Shelf.

4. Discussion

98 Tracing the causes for the southern Weddell Sea salt variability, an additional analysis
99 reveals that pc_1 is strongly correlated with the sea ice concentration and the sea surface
100 salinity (SSS) near the coast at the Greenwich meridian. The SSS anomaly leads pc_1 by

101 up to five years with a correlation $r > 0.5$. Long-term changes of sea ice conditions reflect
102 the influence of the SAM through variable coastal winds. This agrees with a recent study
103 which proposes a link between SAM and the occurrence of the Weddell Polynya [*Gordon*
104 *et al.*, 2007]. From the eastern Weddell Sea the *SSS*-anomaly propagates westward into
105 the central Weddell Sea and onto the southern continental shelf (see also Fig. A2 in the
106 auxiliary material). Here, it influences the stability of the shelf water column such that
107 local air-sea interaction together with sea ice formation and deep convection determine the
108 signal at the sea floor with varying intensity. The shelf circulation carries the signal into
109 the Filchner-Ronne Ice Shelf (FRIS) cavern. However, recirculation, mixing in relatively
110 shallow waters, and ocean-ice shelf interaction damp the signal of the inflowing shelf water
111 in the cavern interior. Therefore, a strong correlation between the S_{bot} -variability and the
112 modeled freshwater flux due to melting at the FRIS base does not exist.

113 The mechanism which transfers the variability from the eastern to the western side of
114 the Antarctic Peninsula is best explained by the results of the sensitivity study. The
115 latter allows the comparison between the impacts of the bottom salinity extremes, solely
116 caused by atmospheric variability in the Weddell Sea sector (see auxiliary material). A
117 saltier (fresher) south/western Weddell Sea is related to a weaker (stronger) zonal density
118 gradient across the western continental shelf break/slope which broadens (narrows and
119 shifts eastward) the core of the western rim current (Fig. 3). As the temperature gradient
120 across the continental slope is large, the shift is related to the transport of colder (warmer)
121 deep waters across the South Scotia Ridge (Fig. 3). The outflow feeds the deep boundary
122 current in southern Drake Passage which extends into the southeast Pacific Ocean thus

123 cooling more (less) the deep layers at the continental slope of the Bellingshausen Sea and
124 beyond.

125 The range of the S_{bot} -variability in the Weddell Sea of this study is comparable to the
126 S -variability found in a 50-year hindcast with BRIOS-2.2 in the Amundsen Sea [*Assmann*
127 *and Timmermann*, 2005]. The Amundsen Sea anomaly propagated primarily westward
128 as part of the Antarctic circumpolar coastal wave [*Beckmann and Timmermann*, 2001].
129 Both publications do not consider a signal transfer from the Weddell Sea into the southeast
130 Pacific Ocean but admit that a thorough analysis of both the atmospheric data and the
131 ocean model results did not happen with regard to this feature. Recent oceanographic
132 observations in southern Drake Passage support the modeled westward flow of Weddell
133 Sea Deep Water [*Naveira Garabato et al.*, 2003], escaping through the gaps in the South
134 Scotia Ridge [*Gordon et al.*, 2001]. Geological records confirm that the deep boundary
135 current continues on the upper continental rise west of the Antarctic Peninsula at least
136 as far as 94°W [*Hillenbrand et al.*, 2003].

5. Conclusions

137 The decadal variability of shelf water salinity in the south/western Weddell Sea inher-
138 ent to our 200-year integration can be related to the periodicity of SAM as part of the
139 model's atmospheric forcing (Fig. 1). The most obvious footprint of the atmospheric signal
140 is the sea ice cover anomaly near the Greenwich meridian strongly influencing sea surface
141 salinity. The Antarctic coastal current provides the link between eastern and southern
142 Weddell Sea. The latter amplifies the surface disturbances and sends out westward prop-
143 agating bottom anomalies which influence the shelf water properties on both sides of the

144 Antarctic Peninsula. Our statistical analysis is supported by the results of the sensitivity
145 study which accentuates the role of the Weddell Sea as dominant source for variability in
146 Antarctic marginal seas. Therefore, an influence from the east should be considered as a
147 new aspect at the present search for mechanisms controlling the flow of warm deep waters
148 towards the floating extensions of the West Antarctic Ice Sheet.

149 **Acknowledgments.** We thank D. Olbers for his contribution to get the project
150 started, C. Wübber and M. Schröter for providing a stable computer performance, and
151 P. Lemke, together with several anonymous reviewers, for a careful reading and helpful
152 comments which significantly improved the original manuscript.

References

- 153 Assmann, K. M., and R. Timmermann (2005), Variability of dense water formation in the
154 Ross Sea, *Ocean Dyn.*, *55*, doi:10.1007/s10236-004-0106-7.
- 155 Beckmann, A., and R. Timmermann (2001), Circumpolar influences on the Weddell Sea:
156 Indication of an Antarctic circumpolar wave, *J. Clim.*, *14*, 3785-3792.
- 157 Coles, V. J., M. S. McCartney, D. B. Olson, and W. M. Smethie Jr. (1996), Changes in
158 Antarctic Bottom Water properties in the western South Atlantic in the late 1980s, *J.*
159 *Geophys. Res.*, *101*, 8957-8970.
- 160 Connolley, W. M., and T. J. Bracegirdle (2007), An Antarctic assessment of IPCC AR4
161 coupled models, *Geophys. Res. Lett.*, *34*, L22505, doi:10.1029/2007GL031648.
- 162 Fahrbach, E., M. Hoppema, G. Rohardt, M. Schröder, and A. Wisotzki (2004), Decadal-
163 scale variations of water mass properties in the deep Weddell Sea, *Ocean Dyn.*, *54*,

- 164 77-91, doi:10.1007/s10236-003-0082-3.
- 165 Gordon, A. L. (1982), Weddell Deep Water variability, *J. Mar. Res.*, *40*, 199-217.
- 166 Gordon, A. L., M. Visbeck, and B. Huber (2001), Export of Weddell Sea deep and bottom
167 water, *J. Geophys. Res.*, *106*(C5), 9005-9017.
- 168 Gordon, A. L., M. Visbeck, and J. C. Comiso (2007), A possible link between
169 the Weddell polynya and the Southern Annular Mode, *J. Clim.*, *20*, 2558-2571,
170 doi:10.1175/JCLI4046.1.
- 171 Hillenbrand, C.-D., H. Grobe, B. Diekmann, G. Kuhn, and D. K. Fütterer (2003), Dis-
172 tribution of clay minerals and proxies for productivity in the surface sediments of the
173 Bellingshausen and Amundsen seas (West Antarctica) - Relation to modern environ-
174 mental conditions, *Marine Geology*, *193*, 253-271.
- 175 Hillenbrand, C.-D., A. Camerlenghi, E. A. Cowan, F. J. Hernández-Molina, R. G. Lucchi,
176 M. Rebesco, and G. Uenzelmann-Neben (2008), The present and past bottom-current
177 flow regime around the sediment drifts on the continental rise west of the Antarctic
178 Peninsula, *Marine Geology*, *255*, 55-63, doi:10.1016/j.margeo.2008.07.004.
- 179 Jacobs, S. S., C. F. Guilivi, and P. Mele (2002), Freshening of the Ross Sea during the
180 late 20th century, *Science*, *297*, 386-389.
- 181 Lefebvre, W., H. Goosse, R. Timmermann, and T. Fichefet (2004), Influence of the
182 Southern Annular Mode on the sea ice-ocean system, *J. Geophys. Res.*, *109*, C09005,
183 doi:10.1029/2004JC002403.
- 184 Naveira Garabato, A. C., D. P. Stevens, and K. J. Heywood (2003), Water mass con-
185 version, fluxes, and mixing in the Scotia Sea diagnosed by an inverse model, *J. Phys.*

- 186 *Oceanogr.*, 33 (12), 2565-2587.
- 187 Rignot, E., and S. S. Jacobs (2002), Rapid bottom melting widespread near Antarctic ice
188 sheet grounding lines, *Science*, 296, 2020-2023.
- 189 Rintoul, S. R. (2007), Rapid freshening of Antarctic Bottom Water formed in the Indian
190 and Pacific oceans, *Geophys. Res. Lett.*, 34, L06606, doi:10.1029/2006GL028550.
- 191 Roeckner, E. (2004), IPCC-AR4 MPI-ECHAM5_T63L31 MPI-OM-GR1.5L40_20C3M
192 run no.1: atmosphere 6 HOUR values MPImet/MaD Germany. CERA-DB "EH5-
193 T63L31_OM-GR1.5L40_20C_1.6H",
194 [http://cera-www.dkrz.de/WDCC/ui/Compact.jsp?acronym=EH5-T63L31_OM-](http://cera-www.dkrz.de/WDCC/ui/Compact.jsp?acronym=EH5-T63L31_OM-GR1.5L40_20C_1.6H)
195 [GR1.5L40_20C_1.6H](http://cera-www.dkrz.de/WDCC/ui/Compact.jsp?acronym=EH5-T63L31_OM-GR1.5L40_20C_1.6H).
- 196 Tarakanov R. Y., M. N. Koshlyakov, E. G. Morozov, and S. V. Gladyshev (2008),
197 Geostrophic currents and water masses in the Drake Passage, Poster, 1607-
198 7962/gra/EGU2008-A-05170.
- 199 Thompson, D. W. J., and S. Solomon (2002), Interpretation of recent Southern Hemi-
200 sphere climate change, *Science*, 296, 895-899.
- 201 Timmermann, R., A. Beckmann, and H. H. Hellmer (2002), Simulation of ice-ocean dy-
202 namics in the Weddell Sea. Part I: model configuration and validation, *J. Geophys.*
203 *Res.*, 107(C3), doi:10.1029/2000JC000741.
- 204 von Storch, H., and F. Zwiers (2003), Statistical analysis in climate research, *Cambridge*
205 *University Press*, Cambridge, UK.
- 206 Walker, D. P., M. A. Brandon, A. Jenkins, J. T. Allen, J. A. Dowdeswell, and J. Evans
207 (2007), Oceanic heat transport onto the Amundsen Sea shelf through a submarine glacial

208 trough, *Geophys. Res. Lett.*, *34*, L02602, doi:10.1029/2006GL028154.

Figure Captions

209 **Figure 1:** Upper: Leading EOF pattern of Southern Ocean bottom salinity south of 50°S
 210 describing $\sim 48\%$ of the variance. Black solid lines represent the model's continental border
 211 including the grounding lines in ice shelf caverns. AP: Antarctic Peninsula; SSR: South Scotia
 212 Ridge. Lower: Corresponding normalized time series (solid line) and 5-year leading Southern
 213 Annular Mode deduced from the ECHAM5-MPIOM forcing (dashed line) for the analyzed period
 214 1920-2099. The correlation of the (5-year shifted) time series amounts to $r = 0.56$. The red
 215 and blue patterns mark years used for the construction of the composite forcing applied in the
 216 sensitivity study (see auxiliary material for a detailed description).

217 **Figure 2:** Upper: Positive (solid lines) and negative (dashed lines) lagged correlations between
 218 the salt anomaly in the southern Weddell Sea and the barotropic streamfunction (Ψ). Colored
 219 lines border areas with a correlation higher $r = 0.5$ ($r_{max} = 0.85$), and colors represent different
 220 lags in time (see insert; positive = salt anomaly leads Ψ). Lower: Regression slope of the
 221 circumpolar bottom temperature (T_{bot}) regressed on the leading S_{bot} -EOF time series (pc_1) for a
 222 positive 4-year time lag (pc_1 leads T_{bot}).

223 **Figure 3:** Bottom distribution of salinity (left), temperature (middle), and velocity (right) in
 224 the Weddell Sea sector for the sensitivity runs forced with the high (upper) and low (lower) at-
 225 mospheric composites (see auxiliary material). Year 2007 and scale were chosen to best represent
 226 the two different phases controlling the flow of deep water out of the Weddell Sea.

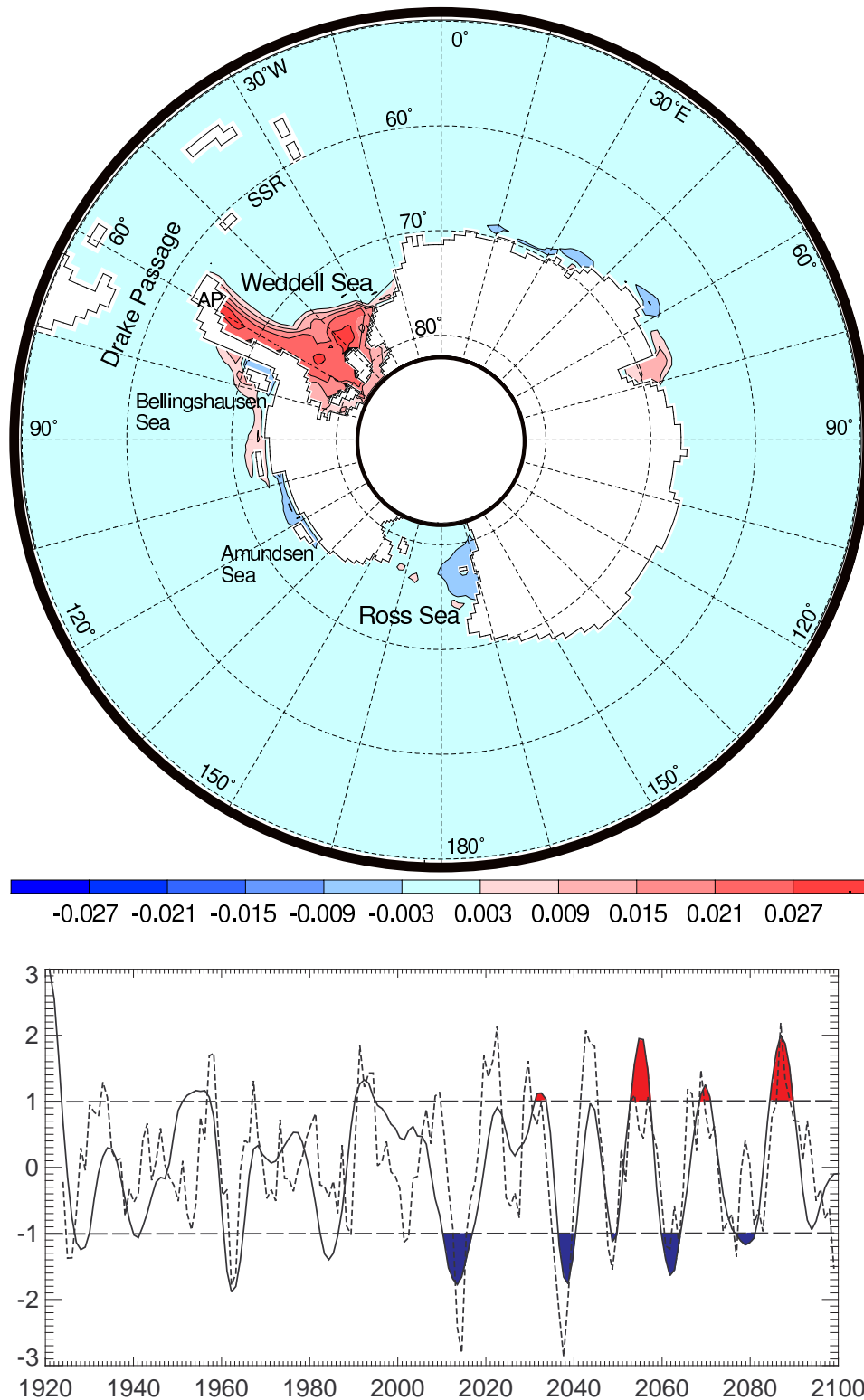


Figure 1. Upper: Leading EOF pattern of Southern Ocean bottom salinity south of 50°S describing ~48% of the variance. Black solid lines represent the model’s continental border including the grounding lines in ice shelf caverns. AP: Antarctic Peninsula; SSR: South Scotia Ridge. Lower: Corresponding normalized time series (solid line) and 5-year leading Southern Annular Mode deduced from the ECHAM5-MPIOM forcing (dashed line) for the analyzed period 1920-2099. The correlation of the (5-year shifted) time series amounts to $r = 0.56$. The red and blue patterns mark years used for the construction of the composite forcing applied in the sensitivity study (see auxiliary material for a detailed description).

D R A F T

March 27, 2009, 1:42pm

D R A F T

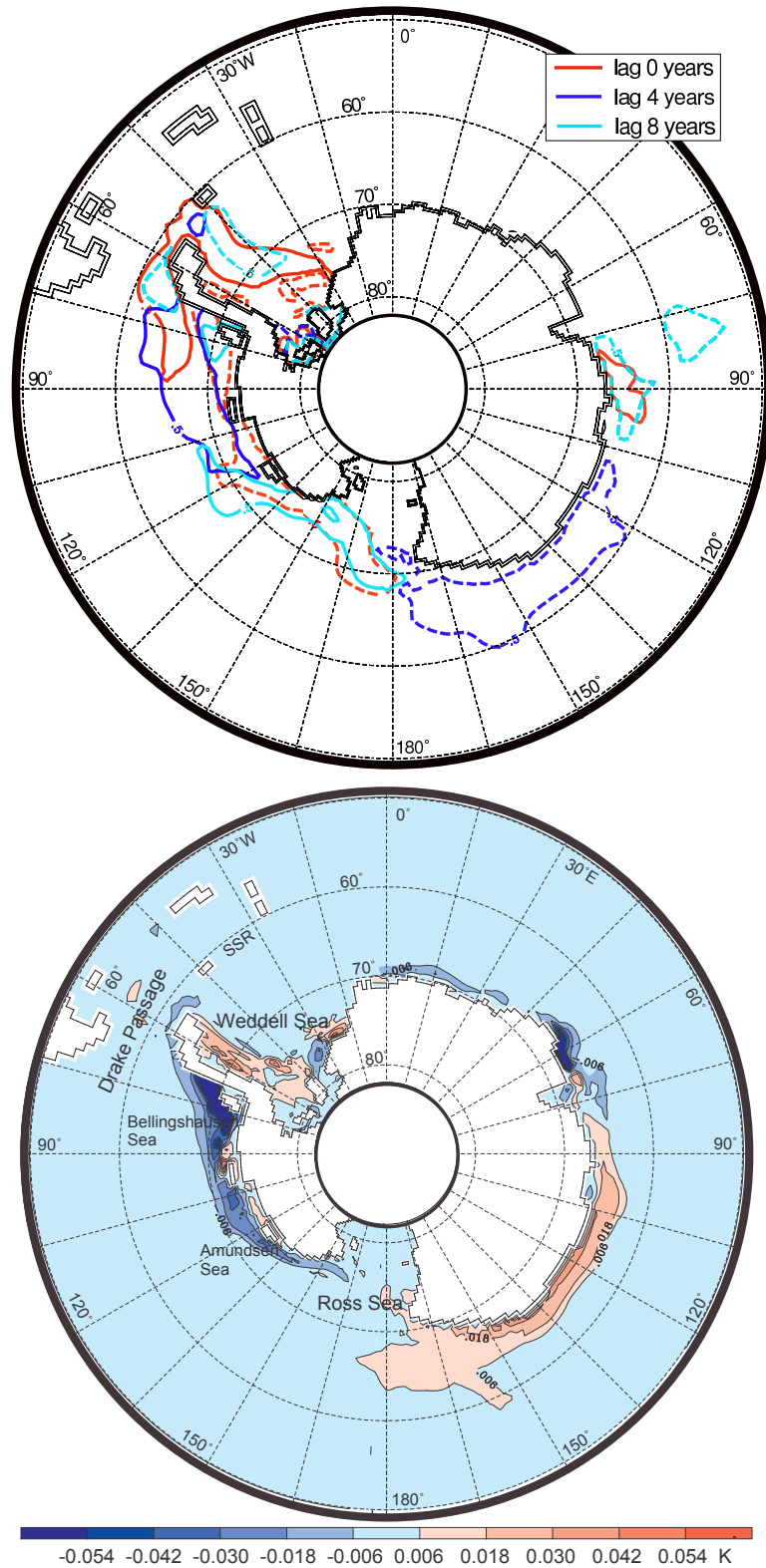


Figure 2. Upper: Positive (solid lines) and negative (dashed lines) lagged correlations between the salt anomaly in the southern Weddell Sea and the barotropic streamfunction (Ψ). Colored lines border areas with a correlation higher $r = 0.5$ ($r_{max} = 0.85$), and colors represent different lags in time (see insert; positive = salt anomaly leads Ψ). Lower: Regression slope of the circumpolar bottom temperature (T_{bot}) regressed on the leading S_{bot} -EOF time series (pc_1) for a positive 4-year time lag (pc_1 leads T_{bot}).

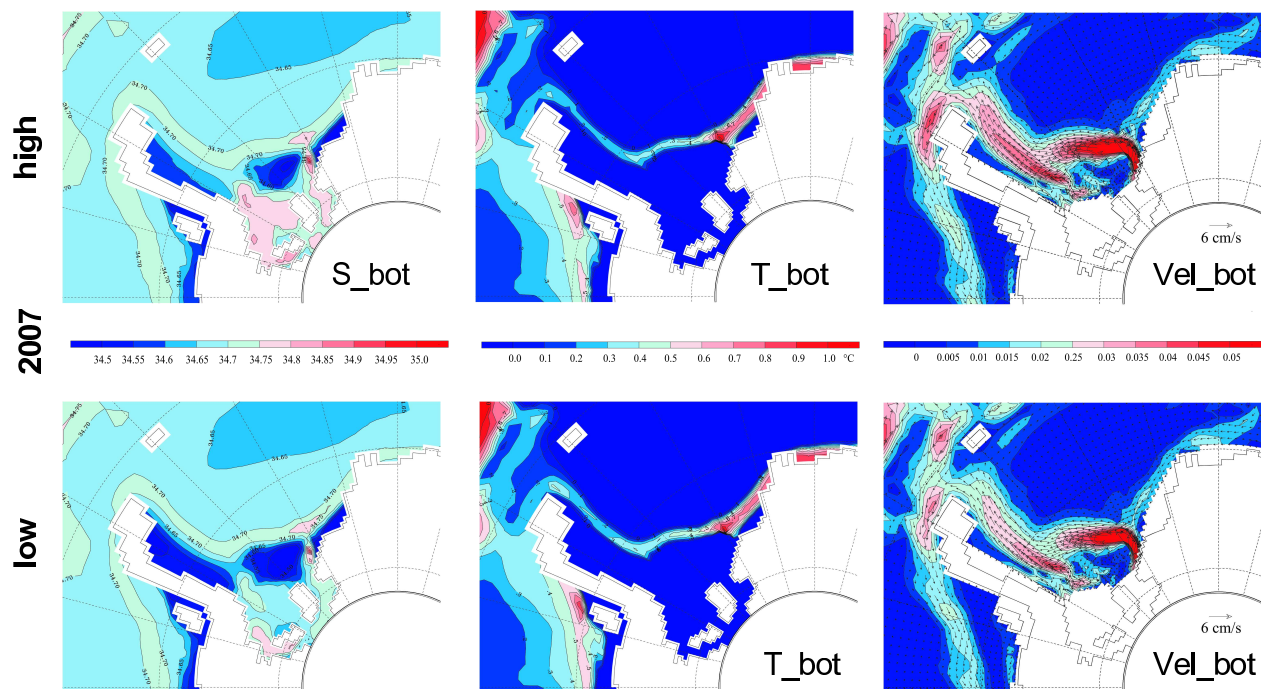


Figure 3. Bottom distribution of salinity (left), temperature (middle), and velocity (right) in the Weddell Sea sector for the sensitivity runs forced with the high (upper) and low (lower) atmospheric composites (see auxiliary material). Year 2007 and scale were chosen to best represent the two different phases controlling the flow of deep water out of the Weddell Sea.